Met. Mater. Int., Vol. 22, No. 3 (2016), pp. 468~473
doi: 10.1007/s12540-016-5603-y

Comparative Study on Microstructure and Martensitic Transformation of Aged Ni-rich NiTi and NiTiCo Shape Memory Alloys

Nader El-Bagoury[1,2,*]

[1]Chemistry Department, Faculty of Science, TAIF University, P.O. Box 888, El-Haweyah, El-Taif, Saudi Arabia
[2]Casting Technology Lab., Manufacturing Technology Dept., Cmrdi, Central Metallurgical Research and Development Institute, P.O. Box 87, Helwan, Cairo, Egypt

(received date: 4 November 2015 / accepted date: 22 January 2016)

In this article the influence of aging heat treatment conditions of 250, 350, 450 and 550 °C for 3 h on the microstructure, martensitic transformation temperatures and mechanical properties of $Ni_{51}Ti_{49}Co_0$ and $Ni_{47}Ti_{49}Co_4$ shape memory alloys was investigated. This comparative study was carried out using X-ray diffraction analysis, scanning electron microscope, energy dispersive spectrometer, differential scanning calorimeter and Vickers hardness tester. The results show that the microstructure of both aged alloys contains martensite phase and Ti_2Ni in addition to some other precipitates. The martensitic transformation temperature was increased steadily by increasing the ageing temperature and lowering the value of valence electron number (e_v/a) and concentration. Moreover, the hardness measurements were gradually increased at first by increasing the aging temperature from 250 to 350 °C. Further elevating in aging temperature to 450 and 550 °C decreases the hardness value.

Keywords: shape memory alloy, microstructure, martensitic transformation, valence electron concentration, hardness property

1. INTRODUCTION

One of the most important and applicable group of alloys that belongs to the functional materials is the shape memory alloys (SMAs), which have attracted much attention because of their superior characteristics, good mechanical properties, and superb corrosion resistance. Among available SMAs, near equiatomic NiTi alloy is regarded as the most workable and useful alloy because of its superelasticity (SE) coupled with the shape memory effect (SME) [1-5].

This nickel-titanium (Nitinol) alloy was firstly developed early in 1960 by W. F. Buehler, a metallurgist investigating nonmagnetic, salt resisting, waterproof alloys for the space programme at the Naval Ordnance Laboratory in Silver Springs, Maryland, USA [6]. It is limited to 100 °C as maximum temperature of martensite transformation temperature (M_s), however it can be elevated with adding a third element such as; Pt, Au, Pd, Hf, Zr and Co with sufficient amount [7-12].

Martensitic transformation temperature is controlled by several factors such as; chemical composition, aging heat treatment conditions, and quenching processes. In aging heat treatment process, time and temperature of heat treatment cycle in addition to the rate of quenching, affect the reverse, and irreversible temperatures of austenitic- martensitic transformation [13].

Fan *et al*. [14] studied the effect of aging on the transformation temperature of martensite and they concluded that M_s increased as the aging time prolonging. For the ternary $Ni_{50.3}Ti_{34.7}Hf_{15}$ shape memory alloy, Javadi *et al*. [15] refer the increment of M_s by about 100 °C after reaching the equilibrium state by the number of valence electrons (e_v/a) and the valence electron concentration (C_v) changes of the Ni-rich NiTi and the Ni-rich NiTiHf alloys that occur during aging treatments. Where they consider two Ni-rich alloys with compositions of $Ni_{50.3}Ti_{49.7}$ and $Ni_{50.3}Ti_{34.7}Hf_{15}$, the calculations of the difference in changes of e_v/a and C_v can be shown as follows [16,17]:

$$e_v/a = f_{Ni}e_v^{Ni} + f_{Ti}e_v^{Ti} + f_{Hf}e_v^{Hf} + \ldots\ldots \quad (1)$$

and

$$C_v^{NiTi} = \frac{e_v}{e_t} = \frac{f_{Ni}e_v^{Ni} + f_{Ti}e_v^{Ti}}{f_{Ni}Z_{Ni} + f_{Ti}Z_{Ti}} \quad (2)$$

and

$$C_v^{NiTiHf} = \frac{e_v}{e_t} = \frac{f_{Ni}e_v^{Ni} + f_{Ti}e_v^{Ti} + f_{Hf}e_v^{Hf}}{f_{Ni}Z_{Ni} + f_{Ti}Z_{Ti} + f_{Hf}Z_{Hf}} \quad (3)$$

*Corresponding author: n.elbagoury@tu.edu.sa

where:

e_v/a: is the number of valence electron per atom of an alloy,

f_{Ni}, f_{Ti} and f_{Hf}: are the atomic fractions in the alloy of Ni, Ti and Hf,

e_v^{Ni}, e_v^{Ti} and e_v^{Hf}: are numbers of valence electrons of Ni, Ti and Hf, and

Z_{Ni}, Z_{Ti} and Z_{Hf}: are atomic number of Ni, Ti and Hf.

The increase or decrease in M_s as a result of alloying is connected with variation in C_v of the alloy. The higher M_s, the lower C_v and vice versa [15,17].

Nishida *et al*. studied the effect of aging conditions on the martensitic transformation behavior in Ni-rich NiTi shape memory alloys and establishing the aging temperature-time diagram for the formation of various Ni-rich precipitates [18] such as Ti_3Ni_4, Ti_2Ni_3 and $TiNi_3$ [19-22]. Others focused on the relationship between the effective aging conditions and the optimum mechanical properties of NiTi SMAs [23-26].

However, to date, such kind of information is scarce about the influence of aging conditions on microstructure, martensitic transformation temperatures, and mechanical properties of NiTiCo shape memory alloy is yet to be established and therefore this is the aim of this research study.

2. EXPERIMENTAL PROCEDURE

Nickel-rich $Ni_{51}Ti_{49}Co_0$ and $Ni_{47}Ti_{49}Co_4$ alloys were manufactured using high-pure Ni, Ti and Co elements via the vacuum arc melting (VAM) process in a water-cooled copper crucible. These alloys were melted four times to ensure homogenization in arc-melting under argon atmosphere. After that both alloys were solutionized at 1000 °C for 24 h. The chemical compositions of the investigated alloys are shown in Table 1. Small-sized parts were taken from each alloy to be used as specimens in the aging heat treatments. These specimens of each alloy were aged at 250, 350, 450 and 550 °C for 3 h, followed by iced water quenching (WQ). The metallographic specimens prepared for the microstructure examination was accomplished according to ASTM E3 [27] then etched in a solution of HNO_3, HF and H_2O in a ratio of 4: 1: 5 respectively to reveal the Ti_2Ni precipitates. To examine the martensite phase, another etching solution of HNO_3/HF/CH_3COOH in a ratio of 4: 4: 2 was used. Microstructural studies using scanning electron microscope (SEM-JEOL JSM5410) was conducted. The equilibrium phase composition was detected by an energy X-ray dispersive spectroscopy (EDS) attached to SEM. The XRD analyses for the crystalline phases in the investigated samples were carried out on a the Brucker axis D8 diffractometer The samples were measured in step scan mode with steps of 0.02° 2θ of range 10-100° using Cu Ka (λ=1.5406) as applied radiation. The martensitic transformation temperatures were measured by differential scanning calorimetry (Netzsch Leading Thermal Analysis DSC 204 F1) at a heating and cooling rates of 10 °C/min. Hardness values were determined using Leco Vickers Hardness Tester LV800AT with 31.25 Kg_f.

3. RESULTS AND DISCUSSION

X-ray diffraction (XRD) is often employed to reveal the crystalline phases. Figure 1 elucidates the XRD patterns of $Ni_{51}Ti_{49}Co_0$ and $Ni_{47}Ti_{49}Co_4$ alloys that aged at different conditions. All the XRD measurements for the investigated eight samples were carried out at room temperature. Each alloy has four XRD pattern according to aging at 250, 350, 450 and 550 °C for 3 h. The main reflected peak in all XRD patterns belongs to the martensite, B19', phase ($L1_0$ structure) in addition to other small diffracted peaks refer to the same phase. Moreover, there are other peaks indicate to the precipitated phases in the microstructure of measured alloys, such as Ti_2Ni, Ni_4Ti_3 and Ni_3Ti phases.

The microstructures of $Ni_{51}Ti_{49}Co_0$ and $Ni_{47}Ti_{49}Co_4$ alloys aged for 3 h at 250, 350, 450 and 550 °C are illustrated in Fig. 2. The microstructures of these aged alloys are consisted of martensite as a matrix and Ti_2Ni precipitates in addition to some other precipitates such as Ni_4Ti_3 and Ni_3Ti, as shown in Fig. 1.

The volume fraction (V_f) and the size of the Ti_2Ni precipitates are affected by two parameters in this study, which are Co content and aging temperature. Compared to the aged $Ni_{47}Ti_{49}Co_4$ alloys, the corresponding $Ni_{51}Ti_{49}Co_0$ alloys have higher V_f of Ti_2Ni precipitates [12]. Moreover, the size of Ti_2Ni particles in $Ni_{51}Ti_{49}Co_0$ alloys is coarser than in the counterpart of $Ni_{47}Ti_{49}Co_4$ alloys. It can be concluded that the Co additions decreased the V_f and the size of Ti_2Ni precipitates, as elucidated in Fig. 2.

The second factor, aging temperature, has a great influence on the V_f, and the size Ti_2Ni precipitates in both $Ni_{47}Ti_{49}Co_4$ and $Ni_{51}Ti_{49}Co_0$ alloys, which affects their mechanical properties. At lower aging temperatures, 250 °C, Ti_2Ni precipitated in lowest V_f and in smallest size among other aged alloys, as

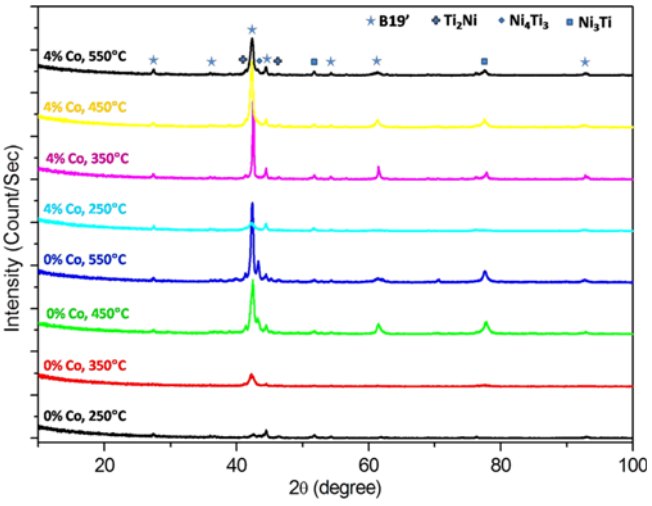

Fig. 1. XRD patterns of the aged $Ni_{51}Ti_{49}Co_0$ and $Ni_{47}Ti_{49}Co_4$ alloys.

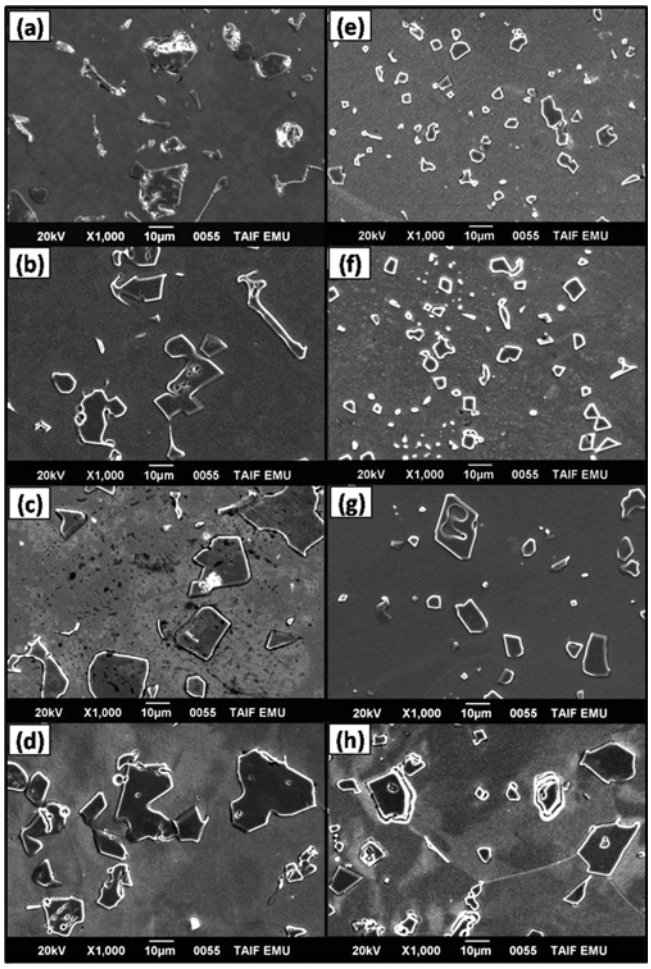

Fig. 2. Microstructure of the aged $Ni_{51}Ti_{49}Co_0$ alloy for 3 h at: (a) 250, (b) 350, (c) 450, and (d) 550 °C and $Ni_{47}Ti_{49}Co_4$ alloy at: (e) 250, (f) 350, (g) 450, and (h) 550 °C.

elucidated in Fig. 2(a) for $Ni_{51}Ti_{49}Co_0$ alloy and in Fig. 2(e) for $Ni_{47}Ti_{49}Co_4$ alloy. By elevating aging temperature to 350 °C, The V_f of the formed Ti_2Ni particles is higher and the size is coarser than in aged alloys at 250 °C, as illustrated in Fig. 2(b) and (f) for 0% Co alloy and for 4% Co alloys, respectively. It seems that, the V_f and the size of the Ti_2Ni particles, precipitated at 350 °C, are the optimum magnitude among all alloys from the mechanical properties point of view as it will be seen later. Further increasing in aging temperatures to 450 and 550 °C leads to an increment in the V_f of Ti_2Ni but remarkably enlarging the Ti_2Ni size, as shown in Fig. 2(c) and (d) for $Ni_{51}Ti_{49}Co_0$ alloys and in Fig. 2(g) and (h) for $Ni_{47}Ti_{49}Co_4$ alloys, respectively. Aging at 550 °C produced the highest V_f and the largest size of the precipitated Ti_2Ni among other alloys. Where the higher aging temperatures increase the mobility of Ti and Ni elements in the matrix to combine forming Ti_2Ni precipitates. These conditions, of high temperatures, enhancing the formation of higher V_f of Ti_2Ni particles and at the same time it allows the small and fine Ti_2Ni precipitates to agglomerate producing coarser size of it.

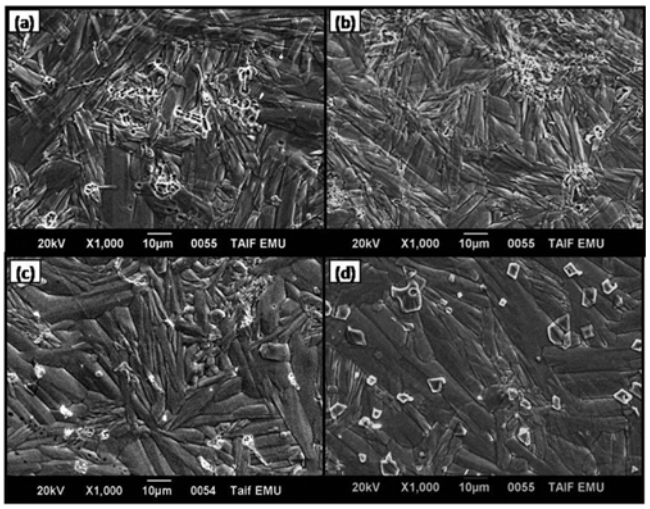

Fig. 3. Martensite phase in the microstructure of $Ni_{51}Ti_{49}Co_0$ alloy aged for 3 h at 250 °C and (b) 550 °C and $Ni_{47}Ti_{49}Co_4$ alloy aged at (c) 250 °C and (d) 550 °C.

In comparison with the aged $Ni_{51}Ti_{49}Co_0$ alloys, the corresponding $Ni_{47}Ti_{49}Co_4$ alloys have lower V_f and smaller size of Ti_2Ni particles, at different aging temperatures. It can be summarized that, at each aging temperature the aged alloys with low Co content have higher V_f and coarser size of Ti_2Ni particles than in the counterpart alloys with high Co content.

The martensitic microstructures of $Ni_{51}Ti_{49}Co_0$ and $Ni_{47}Ti_{49}Co_4$ alloys aged for 3 h at 250 and 550 °C are shown in Fig. 3. The martensitic structure aged at 250 and 550 °C for $Ni_{51}Ti_{49}Co_0$ alloy is elucidated in Fig. 3(a) and (b) and for $Ni_{47}Ti_{49}Co_4$ alloy is shown in Fig. 3(c) and (d), respectively. As a matter of fact that the matrix in all microstructures of aged alloys is fully martensite, it means the transformation temperatures of martensite are higher than the room temperature.

The martensite laths for the aged $Ni_{51}Ti_{49}Co_0$ alloy at 250 °C are thinner than the martensite laths for the same alloy but aged at 550 °C. The same result for the martensite laths was found in the aged $Ni_{47}Ti_{49}Co_4$ alloy after aging at 250 and 550 °C. Additionally the martensite laths for the aged $Ni_{47}Ti_{49}Co_4$ alloys are thicker than that of $Ni_{51}Ti_{49}Co_0$ alloys when compared at the same aging temperature, as shown in Fig. 3. The martensite laths thickness can be used as an evidence of the start of martensite transformation temperature (M_s) of $Ni_{47}Ti_{49}Co_4$ alloys is higher than M_s for the counterpart $Ni_{51}Ti_{49}Co_0$ alloys.

There are different kinds of precipitates can be found in the microstructures of aged $Ni_{51}Ti_{49}Co_0$ and $Ni_{47}Ti_{49}Co_4$ alloys. These precipitates are illustrated in Fig. 4(a) for NiTi, (b) for Ni_4Ti_3 and (c) for Ti_2Ni phases. NiTi precipitates have circular and longitudinal shapes with a chemical composition of 51.16 at% of Ni and 48.84 at% of Ti in $Ni_{51}Ti_{49}Co_0$ alloy aged at 250 °C for 3 h, as elucidated in Fig. 4(a). However, the Ni_4Ti_3 phase is formed in a lenticular shape that consists of 55.46

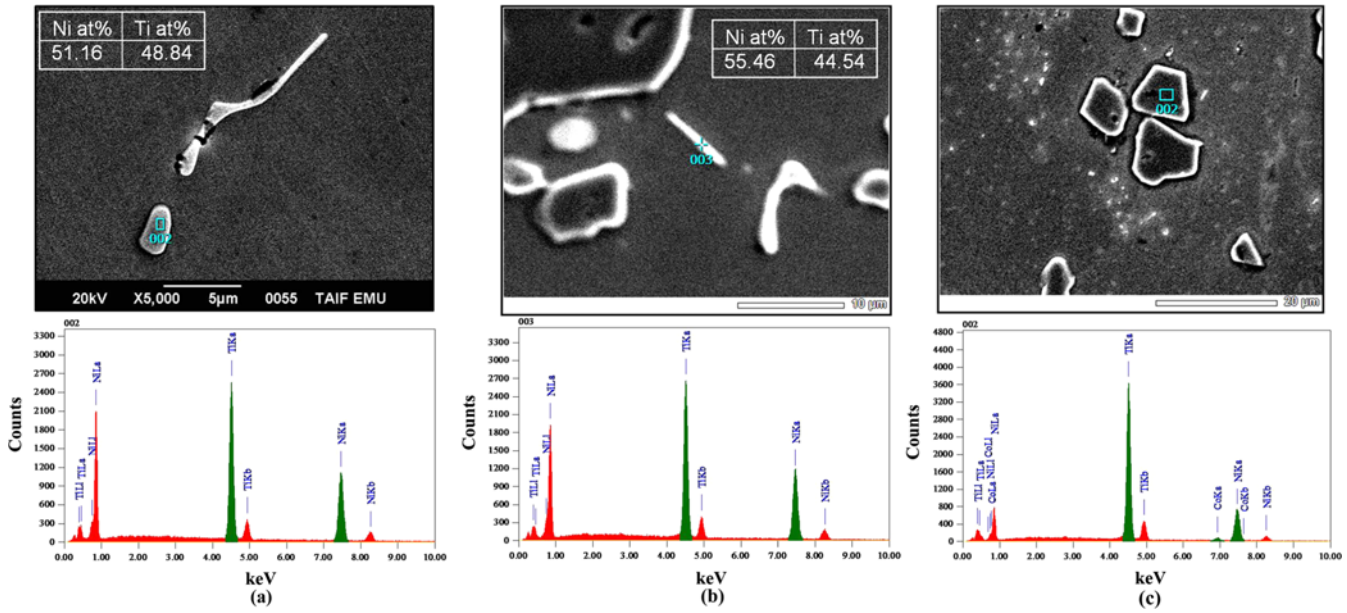

Fig. 4. (a) NiTi precipitate in $Ni_{51}Ti_{49}Co_0$ alloy aged at 250° C for 3 h, (b) Ni_4Ti_3 precipitate in $Ni_{51}Ti_{49}Co_0$ alloy aged at 450 °C for 3 h, and (c) Ti_2Ni precipitate in $Ni_{47}Ti_{49}Co_4$ alloy aged at 350 °C for 3 h.

Table 1. Chemical composition of NiTiCo shape memory alloys

Alloy	Ni, at%	Ti, at%	Co, at%
$Ni_{51}Ti_{49}Co_0$	51.01	48.99	0.00
$Ni_{47}Ti_{49}Co_4$	47.40	48.75	3.85

at% of Ni and 44.54 at% of Ti in in $Ni_{51}Ti_{49}Co_0$ alloy aged at 450 °C for 3 h, as shown in Fig. 4(b). For the Ti_2Ni precipitates, it is found in the microstructures of both aged $Ni_{51}Ti_{49}Co_0$ and $Ni_{47}Ti_{49}Co_4$ alloys with globular shape but in different compositions as illustrated in Table 2. Moreover, the Ni_3Ti can be found as well in the microstructure of investigated aged alloys that aged at higher temperatures such as 550 °C [28,29].

Figure 5 shows the line analysis through Ti_2Ni phase that surrounded by the martensite phase in the microstructure of $Ni_{47}Ti_{49}Co_4$ alloy aged at 450 °C for 3 h. This figure illustrates the distribution of different alloying elements, Ni, Ti and Co, throughout these two phases. The highest line, in red color, represents the distribution of Ti element and the line with green color in the middle shows the distribution of Ni, however the lowest line, in blue color, showing the line analysis of Co element. Obviously, Ti_2Ni phase has higher Ti content than in martensite phase while the martensite phase has higher amount of Ni compared to Ti_2Ni phase. Additionally, Co percentage in Ti_2Ni precipitates is slightly lower than in martensite phase. A comparison between the chemical analyses for Ni, Ti and Co elements in martensite phase and in Ti_2Ni precipitates can be found in Tables 2 and 3. Where Table 2 contains the chemical composition of Ni, Ti and Co in Ti_2Ni particles and Table 3 includes the percentages of the three elements in the martensite phases of aged alloys.

In addition to the chemical analysis of martensite phases,

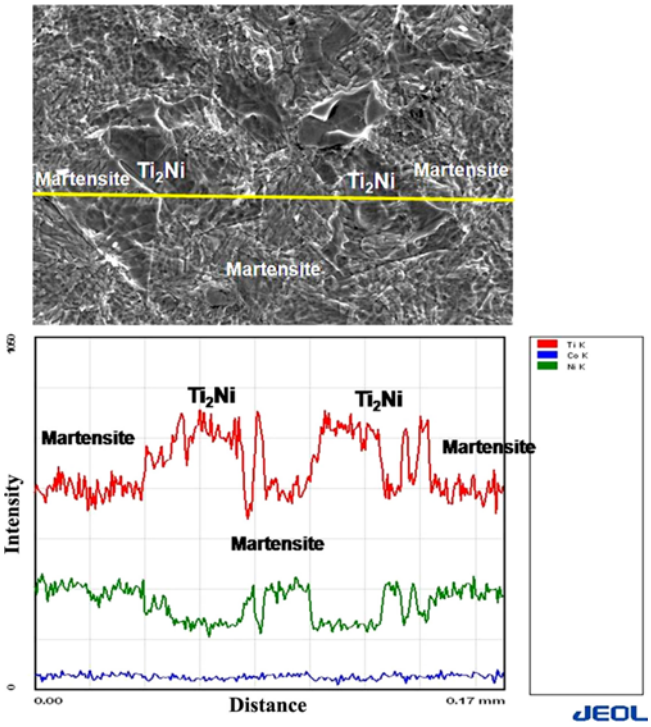

Fig. 5. Line scanning through Ti_2Ni precipitate and martensite phase in $Ni_{47}Ti_{49}Co_4$ alloy aged at 450 °C for 3 h.

Table 2. Chemical composition of Ti_2Ni in $Ni_{51}Ti_{49}Co_0$ and $Ni_{47}Ti_{49}Co_4$ alloys

Alloy	Composition (at%)		
	Ni	Ti	Co
$Ni_{51}Ti_{49}$	33.63	66.37	0.00
$Ni_{47}Ti_{49}Co_4$	32.54	65.19	2.27

Table 3. Chemical composition of martensite in different aged alloys, C_v, e_v/a and M_s

Alloy	Composition of martensite, (at%)			C_v	e_v/a	M_s (°C)
	Ni	Ti	Co			
0% Co, 250 °C	53.24	46.76	0.00	0.28556	7.1944	47
0% Co, 350 °C	52.92	47.08	0.00	0.28501	7.1752	59
0 % Co, 450 °C	52.77	47.19	0.00	0.28479	7.1646	70
0% Co, 550 °C	52.64	47.36	0.00	0.28453	7.1584	79
4% Co, 250 °C	48.35	48.26	3.39	0.26229	7.0027	74
4% Co, 350 °C	48.13	48.42	3.45	0.26168	6.9913	81
4 % Co, 450 °C	47.83	48.59	3.58	0.26066	6.9772	94
4% Co, 550 °C	47.69	48.67	3.64	0.26019	6.9706	107

Table 3 contains the start of martensistic transformation temperature (M_s), C_v and e_v/a values for each aged alloy. Table 3 reveals that the martensitic transformation temperatures can be greatly affected by aging temperature. It is obvious that the M_s values are increased as the aging temperatures elevate in both $Ni_{51}Ti_{49}Co_0$ and $Ni_{47}Ti_{49}Co_4$ alloys. By increasing the aging temperature and Co additions at the expense of Ni, Ni content depresses in the matrix of the investigated alloys elevating the value of M_s as achieved by Lekston *et al*. [30]. Variation in the Ni composition of the matrix governs the transformation temperatures as reached by Frenzel *et al*. [31]. Therefore M_s measurements for $Ni_{47}Ti_{49}Co_4$ alloys are higher than that for $Ni_{51}Ti_{49}Co_0$ alloys as reflected in Table 3. Moreover a clear correlation between M_s and C_v and e_v/a is found.

Both of C_v and e_v/a were calculated using Zarinejad and Liu [16,17] equations No. 1, 2 and 3 mentioned in the introduction section. The number of valence electrons are usually considered as the number of d and s electrons for an atom of transition metals, and p and s electrons for an atom for non-transition ones [16]. The following configurations of the valence electron per atom were used; for Ni: [Ar] $3d^8$ $4s^2$ [32]; for Ti: [Ar] $3d^2$ $4s^2$ [4] and for Co: [Ar] $3d^7 4s^2$ [33].

As illustrated in Table 3, there is an inverse relationship between M_s from one side and C_v and e_v/a on the other side. The results of the present study show that the relation of e_v/a and M_s are in a good agreement with the results obtained by Wang *et al*. [34] and also de Arago *et al*. [35].

The M_s measurement range is lying between 47 °C and 107 °C as shown in Table 3. The lowest value of M_s, 47 °C, was found in $Ni_{51}Ti_{49}Co_0$ alloy aged at 250 °C for 3 h. While the highest magnitude for the M_s, 107 °C, was achieved in $Ni_{47}Ti_{49}Co_4$ alloy aged at 550 °C after 3 h.

The influence of the aging conditions on the mechanical properties of $Ni_{51}Ti_{49}Co_0$ and $Ni_{47}Ti_{49}Co_4$ alloys was studied. Hardness property of aged $Ni_{51}Ti_{49}Co_0$ and $Ni_{47}Ti_{49}Co_4$ alloys was used as the reference for the mechanical properties. Hardness measurements were carried out according to ASTM standard E92-03 [36]. As shown in Fig. 6, the hardness measurements of $Ni_{51}Ti_{49}Co_0$ and $Ni_{47}Ti_{49}Co_4$ alloys plotted against aging temperatures.

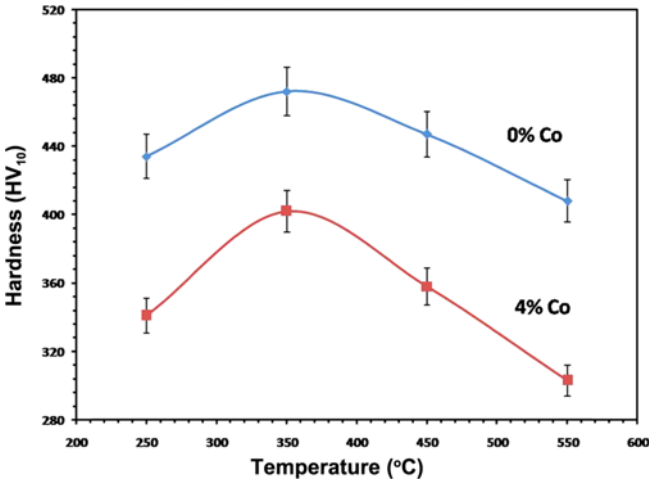

Fig. 6. Hardness measurements for aged $Ni_{51}Ti_{49}Co_0$ and $Ni_{47}Ti_{49}Co_4$ alloys.

Hardness values for the $Ni_{51}Ti_{49}Co_0$ alloys are higher than the corresponding $Ni_{47}Ti_{49}Co_4$ alloys as illustrated in Fig. 6. In both alloys, at first, the hardness increases with elevating aging temperature from 250 °C to 350 °C, which has the optimum hardness value. As the aging temperature increased to 450 °C, the hardness decreased. Further decrease in hardness measurement was achieved when the aging temperature increased to 550 °C. The highest hardness value gained with aging at 350 °C; however the lowest hardness obtained at 550 °C aging temperature, as shown in Fig. 6.

The V_f of the hard Ti_2Ni precipitates in the microstructures of $Ni_{51}Ti_{49}Co_0$ alloy is higher than in the counterpart microstructures of $Ni_{47}Ti_{49}Co_4$ alloy. Additionally, the size of these precipitates is smaller in the Co contained alloys in comparison with the Co free alloys. As a result of elevated M_s for the 4% Co alloy than for the 0% Co, as shown in Table 3, the martensite phase of the $Ni_{51}Ti_{49}Co_4$ alloy has coarse lath than the martensite lath in $Ni_{47}Ti_{49}Co_0$ alloy. Therefore, the hardness measurements for 4% Co alloy are lower than the hardness values for the 0% Co alloy.

By raising the aging temperature for both investigated alloys from 250 to 350 °C, the V_f in addition to the size of the Ti_2Ni

reached the combined optimum magnitude, as demonstrated in Fig. 2. These ideal conditions of V_f and size of Ti_2Ni interpret the highest hardness value achieved at 350 °C. Further increasing in aging temperatures to 450 and then to 550 °C, resulting in enlarging in the size of the Ti_2Ni phase compared to the size of Ti_2Ni phase found in the microstructure the alloys aged at 250 and 350 °C, as shown in Fig. 2. Moreover, the thickness of the martensite lath played an additional role, where the martensite lath after aging at 450 and 550 °C is thicker than the martensite lath after aging at 250 and 350 °C in both investigated alloys, as shown in Fig. 3.

Therefore the hardness values obtained for the samples aged at 450 and 550 °C were deteriorated especially for the latter one, which had the lowest hardness measurement.

4. CONCLUSION

The influence of aging treatment on the microstructure and martensitic transformation temperatures as well as on the mechanical properties of $Ni_{51}Ti_{49}Co_0$ and $Ni_{47}Ti_{49}Co_4$ alloys was studied and the results can be addressed as follows:

(1) The microstructure of both $Ni_{51}Ti_{49}Co_0$ and $Ni_{47}Ti_{49}Co_4$ alloys, aged at various temperatures for 3 h, consists of martensite and some precipitates of Ti_2Ni, Ni_4Ti_3 and Ni_3Ti.

(2) The V_f and the size of Ti_2Ni in addition to the martensite lath increase as the aging temperature elevates in both alloys. Compared to $Ni_{47}Ti_{49}Co_4$ alloys, the corresponding $Ni_{51}Ti_{49}Co_0$ alloys have higher V_f and coarser size of Ti_2Ni particles.

(3) M_s values of $Ni_{51}Ti_{49}Co_0$ alloys increases with the aging temperatures and Co content (4% at.). M_s has an inverse relationship with both of C_v and e_v/a.

(4) The highest hardness value for both $Ni_{51}Ti_{49}Co_0$ and $Ni_{47}Ti_{49}Co_4$ alloys obtained after aging at 350 °C for 3 h. $Ni_{51}Ti_{49}Co_0$ alloys have higher hardness values in comparison with counterpart $Ni_{47}Ti_{49}Co_4$ alloys at each aging temperature.

REFERENCES

1. K. Otsuka and C. M. Wayman, *Shape Memory Materials*, p. 516, Cambridge University Press, UK (1998).
2. A. Mehta, V. Imbeni, R. O. Ritchie, and T. W. Duerig, *J. Mat. Sci. Eng. A* **378**, 130 (2004).
3. H. Matsumoto, *J. Mater. Sci. Lett.* **11**, 367 (1992).
4. N. El-Bagoury and A. A. Nofal, *J. Mater. Sci. Technol.* **30**, 982 (2014).
5. K. M. Ibrahim, N. Elbagoury, and Y. Fouad, *J. Alloy. Compd.* **509** (2011) 3913.
6. W. H. Buehler, J. V. Gilfrich, and R. C. Wiley, *J. App. Phys.* **34** (1963) 1475.
7. D. N. Abujudom, P. E. Thoma, M.-Y. Kao, D. R. Angst, *US patent No. 5*, **114**, 504 (1992).
8. X. D. Han, W. H. Zou, S. Jin, Z. Zhang, and D. Z. Yang. *J. Scr. Metall. Mater.* **32**, 1441 (1995).
9. K. H. Eckelmeyer. *Scr Metall* **10**, 667 (1976).
10. Y. C. Lo, S. K. Wu, and C. M. Wayman. *J. Scr. Metall. Mater.* **24**, 1571 (1990).
11. P. E. Thoma and J. J. Boehm. *J. Mater. Sci. Eng. A* **273-275**, 385 (1999).
12. N. El-Bagoury, *J. Mater. Sci. and Tech.* **30**, 1795 (2014).
13. K. W. K. Yeunga, K. M. C. Cheunga, W. W. Lua, and C. Y. Chungb, *J. Mater. Sci. Eng. A* **383**, 213 (2004).
14. G. Fan, W. Chen, S. Yang, J. Zhu, X. Ren, and K. Otsuka. *J. Acta Mater.* **52**, 4351 (2004).
15. M. M. Javadi, S. H. Seyedein, M. T. Salehi, and M. R. Aboutalebi, *J. Acta Mater.* **61**, 2583 (2013).
16. M. Zarinejad and Y. Liu. *Chapter 12, Dependence of Transformation Temperatures of Shape Memory Alloys on the Number and Concentration of Valence Electrons in: Shape Memory Alloys: Manufacture, Properties and Applications* (ed. H. R. Chen), p. 341, Nova Science Publishers (2010).
17. M. Zarinejad and Y. Liu. *J. Adv Funct. Mater.* **18**, 2789 (2008).
18. M. Nishida, C. M. Wayman, and T. Honma. *J. Metall. Trans. A* **17**, 1505 (1986).
19. Y. F. Zheng, F. Jiang, L. Li, H. Yang, and Y. Liu. *J. Acta Mater.* **56**, 736 (2008).
20. M. Nishida, C. M. Wayman, R. Kainuma, and T. Honma. *J. Scripta Mater.* **20**, 899 (1986).
21. T. Hara, T. Ohba, K. Otsuka, and M. Nishida, *J. Mater. Trans. JIM* **38**, 277 (1997).
22. M. Nishida, C. M. Wayman, and T. Honma. *J. Metall. Trans. A* **18**, 285 (1987).
23. S. Miyazaki, T. Imai, Y. Igo, and K. Otsuka. *J. Metall. Trans. A* **17**, 115 **(**1986).
24. K. Otsuka, K. Shimizu. *J. Scripta Metall.* **4**, 469 (1970).
25. K. Otsuka, C. M. Wayman In: K. Otsuka, and Wayman, *Shape Memory Materials*, p. 27, Cambridge University Press, UK (1998).
26. K. Otsuka, C. M. Wayman, K. Nakai, H. Sakamoto, and K. Shimizu, *J. Acta Metall.* **24**, 207 (1976).
27. ASTM Standard E3. *Standard Practice for Preparation of Metallographic Specimens*, ASTM Digital Library (1995).
28. N. El-Bagoury, *J. Mater. High Temp.* **32**, 390 (2015).
29. K. Otsuka and X. Ren, *J. Mater. Sci.* **50**, 511 (2005).
30. Z. Lekston and E. Tagiewka. *J. Arch. Mater. Sci. Eng.* **28**, 665 (2007).
31. J. Frenzel, E. P. George, A. Dlouhy, C. Somsen, M. F.-X. Wagner, and G. Eggeler, *J. Acta Mater.* **58**, 3444 (2010).
32. V. A. Chernenko. *J. Scr. Mater.* **40**, 523 (1999).
33. http://www.oneonta.edu/faculty/viningwj/Chem111/Chapter07.pdf (accessed March 14, 2015).
34. R. L. Wang, J. B. Yan, H. B. Xiao, L. S. Xiao, V. V. Marchenkov, L. F. Xu, and C. P. Yang, *J. Alloy. Compd.* **509**, 6834 (2011).
35. C. J. de Arajo, N. J. da Silva, M. M. da Silva, and C. H. Gonzalez, *J. Mater. Des.* **32**, 4925 (2011).
36. ASTM Standard E92-03, *Standard Test Methods for Vickers Hardness of Metallic Materials*, ASTM Digital Library (2003).